

ANALYSIS OF VOID MORPHOLOGY AND DISTRIBUTION IN NATURAL FIBER REINFORCED COMPOSITES

Madra, A^{1,2*}, Dan-Thuy, VP³, Breitkopf, P², Trochu, F¹

¹ Mechanical Engineering Department, CREPEC, École Polytechnique de Montréal, Canada

² Laboratoire Roberval, UMR 7337 UTC-CNRS, Université de Technologie de Compiègne, France

³ Department of Chemical Engineering, Can-Tho University, Can Tho City, Vietnam

* Corresponding author (annakopov@gmail.com)

Keywords: *X-ray microtomography, natural fibers, microstructural analysis*

ABSTRACT

A computational approach with deep learning architecture is proposed to the quantitative analysis of defects in composites. X-ray microtomographic scans provide information on the three-dimensional geometry of residual voids and cracks present in the experimental microstructure. Their signature is retrieved by casting 3D geometrical features to the deep feature space learned with the feed-forward multilayer artificial neural network. Morphological classes are determined by clustering deep features, and their spatial distribution is then further analyzed. The spatial clusters with the similar morphological composition are identified, thus providing a descriptor for the defect geometry and distribution, required for quantitative comparison of microstructures. The methodology is presented for a composite of acrylonitrile butadiene styrene (ABS) reinforced with unidirectional banana fibers.

1 INTRODUCTION

The general assessment of the efficiency of a manufacturing method can be performed by either verification of the mechanical performance of the produced part or by destructively or non-destructively characterizing defects present in the material. In the latter case, the traditional approach to defect control is based on comparison between the actual experimental microstructure of the material and its theoretical idealized model. In the context of fiber reinforced polymeric matrix composites, this process concentrates on establishing the weight fraction of residual voids according to the ASTM D2734 - 16 [1] standard, which relies on composite density measurement prior and post matrix incineration or digestion. This technique gives a global view of the weight fractions of the phases in the material, but its accuracy is limited to macroscale defects and does not provide any indications on the morphology of defects.

Alternatively, various planar imaging techniques, ranging from optical microscopy to Scanning Electron Microscopy (SEM) can be employed. Their advantage lies in the higher resolution, permitting the identification of microscale details, as well as in providing insight to the geometrical form and distribution of defects in the material. The

quantitative analysis of morphology can be performed with techniques developed for quantitative metallography, usually concentrating on such geometric features of defects like diameter, area, length or tortuosity.

The limitation to two dimensions may be further overcome by applying X-ray microtomography which yields phase-relative information in the volume of the specimen. Several approaches to measuring geometrical parameters of defects have been proposed [9, 6], as well as to characterize their spatial distribution [7]. Due to the high complexity of geometric forms of different types of defects, the joint analysis of morphology and spatial distribution of defects remains an open problem. To enable comparisons between different spatial clusters of defects, efficient descriptors of their morphology need to be identified. Here, we would like to present an approach to determining such descriptors from X-ray microtomographic scans. The methodology presented relies on a deep learning architecture employing a combination of fast-forward multilayer neural networks to reduce the dimensionality of the classification problem and increase the separability of potential morphological classes. Following the assignment of morphological classes to the individual defect geometries is the analysis of their spatial distribution and identification of spatial clusters with analogical morphological constitution. The method is applied to a banana fiber reinforced thermoplastic, thus introducing an additional difficulty of organic geometry of natural fibers to the problem.

2 EXPERIMENTAL METHODS

2.1 Materials

The composite was manufactured by compression molding at the Department of Chemical Engineering of Can-Tho University, Vietnam. Long fibers extracted from banana leaves were placed in eight unidirectional layers, amounting to a 40% weight fraction. Acrylonitrile butadiene styrene (ABS) thermoplastic was used as matrix. The alternating layers of polymer and thermoplastic were compressed for 20 minutes under pressure $P = 9.8$ MPa at a temperature $T = 170^\circ\text{C}$.

2.2 X-ray microtomography

The specimen for the analysis was cut out from the central part of the manufactured sheet. The dimensions of the scanned part of the specimen were: width=0.3, height=0.5, and depth=1.2 mm. The X-ray microtomography was performed on a FLEX-M863-CT X-ray microtomograph from Beamsense Co. Ltd. at the Kyoto Institute of Technology, Kyoto, Japan. The tomograms were reconstructed with filtered back-projection algorithm after elimination of ring artifacts and removal of illumination fluctuation. The voxel resolution of the reconstructed tomograms was $1.7 \mu\text{m}$.

2.3 Image preprocessing

Untreated tomograms (Fig. 1a) contain information about the spectrum of attenuation coefficients μ , proper for each phase in the microstructure. Based on the spectrum of μ and its convolutions with Gaussian, Sobel and Hessian kernels, a Fast Random Forest (FRF) algorithm [2] was trained to discern three types of phases: fibers, matrix and air, resulting in a segmented tomogram (Fig. 1b). Further convolution with Sobel kernel yielded outlines of fiber and air phases, then transformed into triangular three-dimensional surface mesh (Fig. 2). Further treatment will be performed on the 3D mesh of the air phase confined to the scanned specimen, thus representing defects of the microstructure.

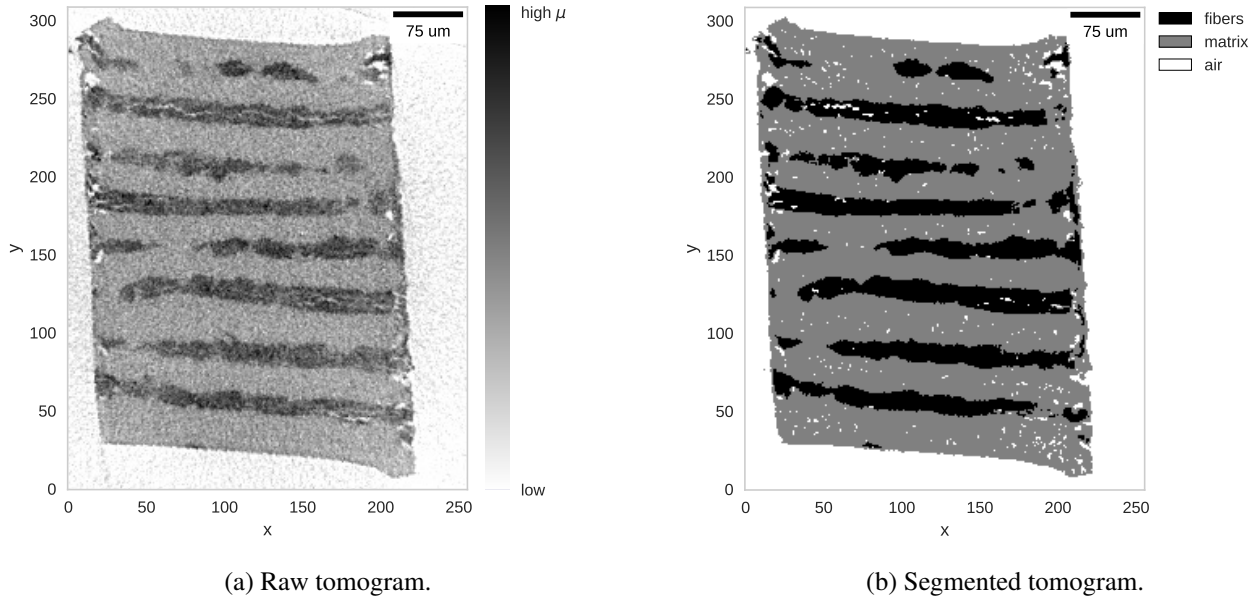


Figure 1: X-ray microtomographic scan (a) before and (b) after phase segmentation; μ is the coefficient of attenuation.

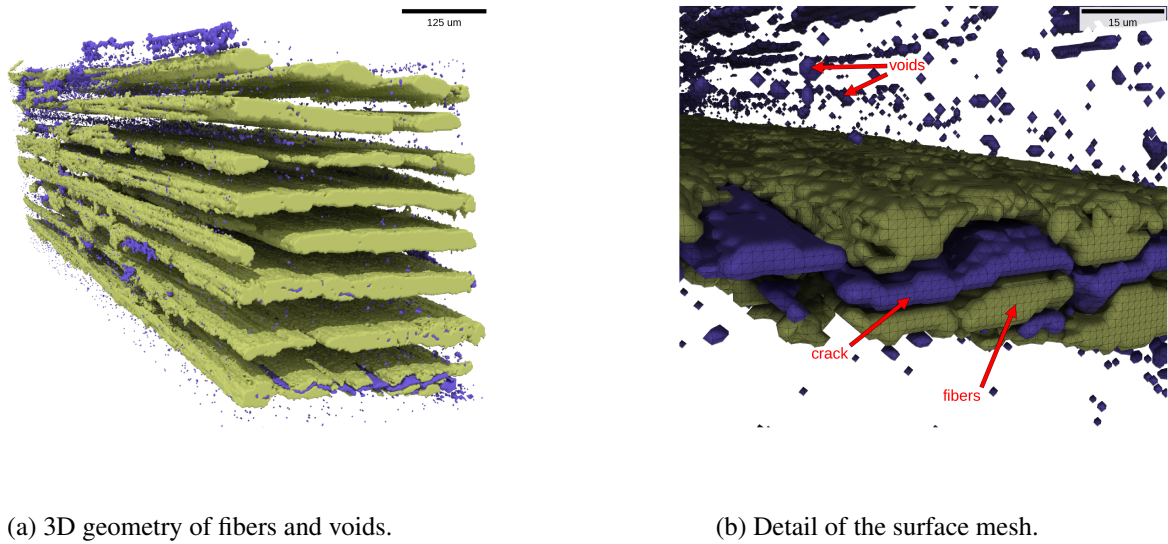


Figure 2: Reconstructed geometry of fibers and voids: (a) global view of the geometry; (b) detail of the triangular surface mesh.

3 MORPHOLOGY CLASSIFICATION

The methodology for retrieving the signature of defects is composed of three parts: extraction of geometric features, classification of morphological types, and identification of spatial clusters. These steps will be outlined in the following subsections and are documented in other works of the authors [6, 8].

3.1 Feature extraction

The three-dimensional geometric features have been extracted using algorithms developed by the authors in [6]. The surface mesh of each defect has been measured providing the volume, surface, aspect ratio and maximal dimensions in orthogonal directions (indicated in Fig. 3). Additionally, the spatial coordinates of the centroid position have been retrieved. Defects with a volume smaller than one voxel³ were eliminated on account of being potential noise.

3.2 Classification of morphology

To reduce the scale of the problem, a correlation analysis has been performed on geometric features to identify potential dependency. A scatterplot in Fig. 4 shows a strong correlation between volume and surface, which display unimodal distributions with a long tail towards maximum values. Other geometric features do not show any correlation and have multimodal distributions. Since the aspect ratio is calculated as the ratio of the two largest dimensions, the following features are sufficient for the classification task: volume, height, width and depth.

The space of geometric features has four dimensions and standard clustering approaches like K-means [4] or Multi-Dimensional Scaling (MDS) [5] do not provide satisfying results. We propose the use of feed-forward multilayer artificial neural network [11], as described in [8] to further reduce the dimensionality of the problem. The deep learning architecture was designed in *Python* with the help of *Scikit-learn* [10] and *H₂O* [3] and consisted of two layers, yielding three deep features learned from the initial set of four geometric features. The classification of

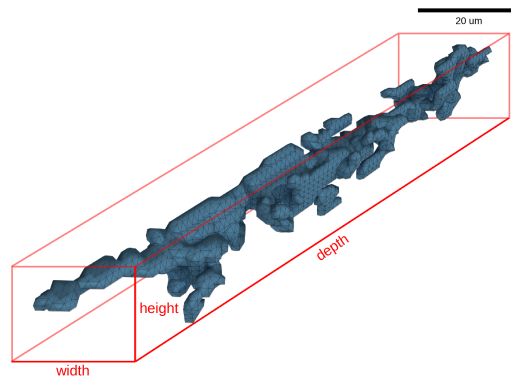


Figure 3: Three-dimensional geometric features of voids.

morphology was then performed on deep features with K-means clustering algorithm. The number of detected classes was calibrated by calculating Bayesian information criterion (BIC) for $N = 20$ clustering models for numbers of classes $M = 2, 3, \dots, 20$. The smallest number of classes close to the 25th percentile of the BIC results was chosen. This step reduces the possibility of model overfitting. The optimal clustering model was then used to assign a morphology class to each defect.

3.3 Analysis of spatial distribution

Contrary to the geometric features, the analysis of spatial distribution is reduced to the three-dimensional Euclidean space of centroid coordinates of each defect. Similarly to the morphology classification, the choice of clustering model was calibrated with BIC for $N = 20$ models and $M = 2, 3, \dots, 30$ classes. The identified spatial clusters of defects were analyzed statistically to determine the proportional volume fraction of morphological classes. The morphological composition of each cluster was then used to perform comparisons.

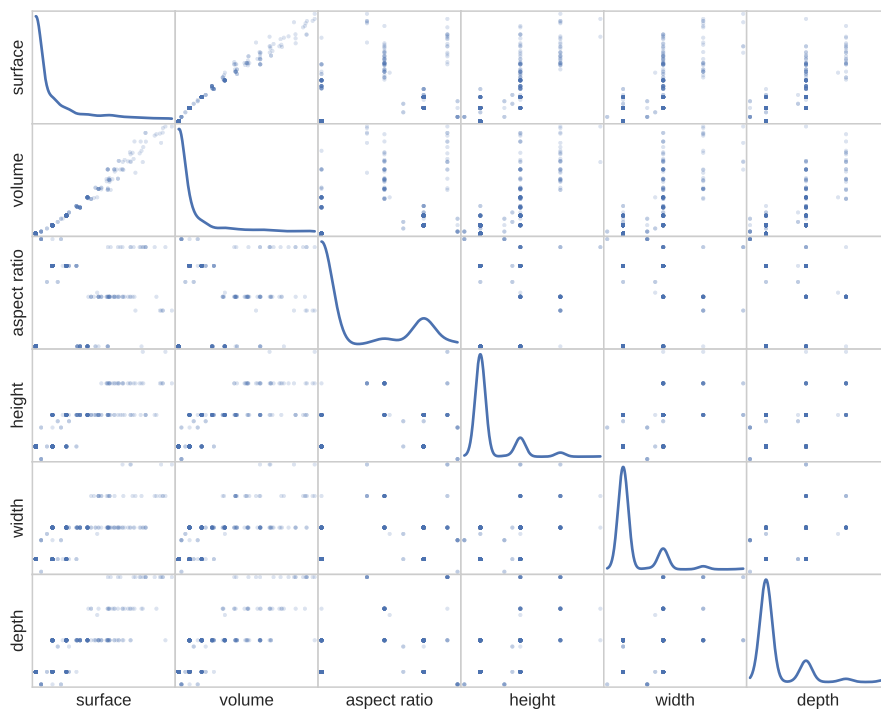


Figure 4: Scatterplot matrix for geometric features. Kernel density estimation on diagonal.

4 RESULTS AND DISCUSSION

The methodology described in Section 3 was applied to a set of 33 758 objects, from which 21 771 were retained. A set of 11 987 objects was removed from the analysis on account of volume smaller than 1 voxel³ or being mostly located above the surface of the specimen. The filtering was necessary to include in the analysis the open cracks, but remove the geometry resulting from surface rugosity. The clustering of deep feature space learned from the geometric features of the retained set is presented in Fig. 5. A total of $k_m = 10$ morphological classes were observed, with a separate class #10 for a large crack indicated in Fig. 6, which was removed from the training set to reduce the skew it induced. Examples of two morphological classes are presented in Fig. 7a and 7b together with histograms of volume and aspect ratio within each class. It can be noted, that despite low volume, defects identified as morphology class #4 constitute as much as 10% of the entire volume of defects. This points to the importance of objective, quantitative approach in the analysis of the composition of microstructures, as this type of morphology is usually omitted in manual analyses.

The spatial clustering has yielded $k_s = 20$ distinct clusters. Their composition is illustrated in Fig. 8. Despite variability, some patterns can be discerned, e.g., the proportional composition of clusters #4, 13 and 14 is very similar, indicating an agglomeration of defects with analogical volume percentage of distinct morphological classes. Analogies are also present for clusters #2, 15 and 17, as well as for #8 and 19.

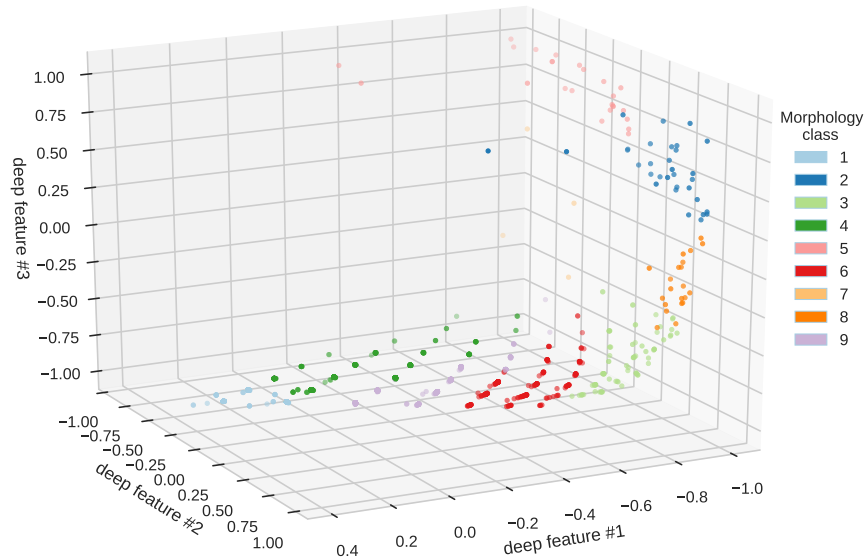


Figure 5: Learned deep features with identified morphological classes.

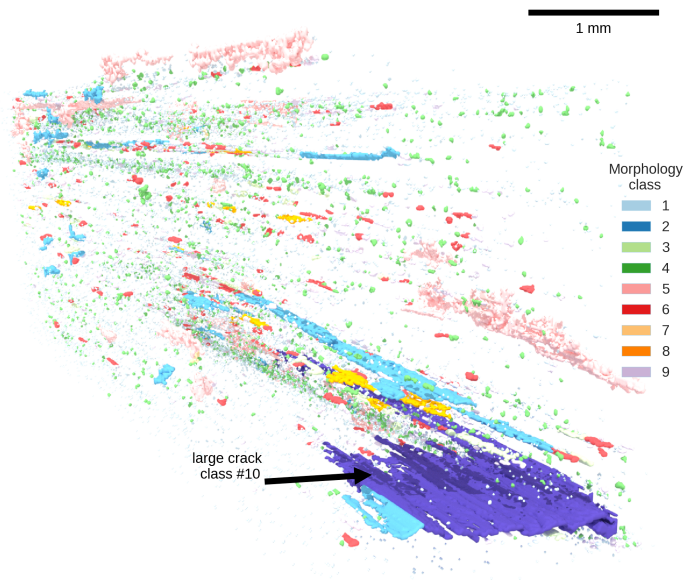


Figure 6: 3D geometry of defects with identified morphological classes.

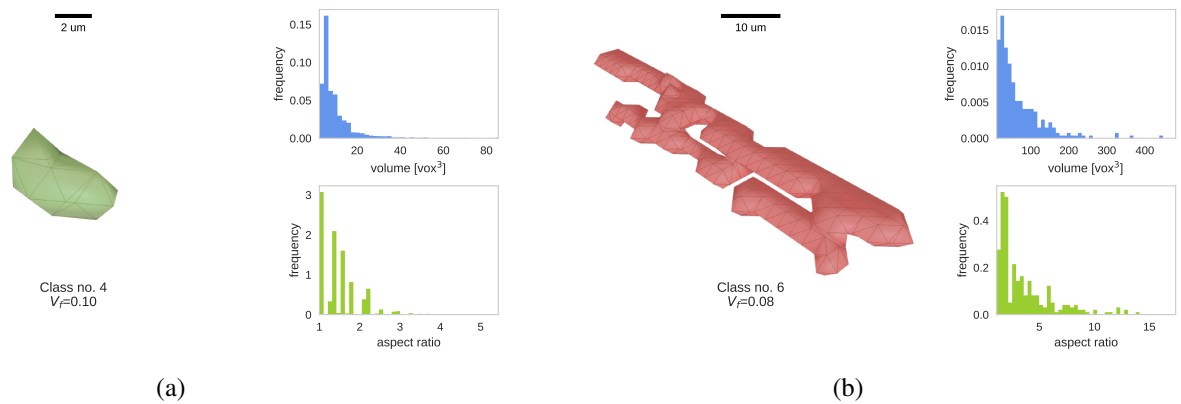


Figure 7: Examples of identified morphological classes with the range of values of their geometrical features: (a) class no. 4; (b) class no. 6.

5 CONCLUSIONS

The X-ray microtomographic scan of experimental microstructure of a complex material has been transformed into a set of individual, three-dimensional geometries of defects, classified into morphological classes and spatial clusters. The deep learning architecture allowed to minimize the involvement of the human operator, thus reducing bias in the analysis of complex geometry. A similar proportional volume fraction of morphological classes in the spatial clusters of defects has been observed for distinct groups of defects. This implies the existence of similar configurations of defects, and can be treated as a signature describing the microstructure. Such descriptors can be used for correlating manufacturing parameters with the morphology and distribution of residual voids or for comparing fracture mechanisms. The exploration of these applications is the subject of ongoing works of the authors.

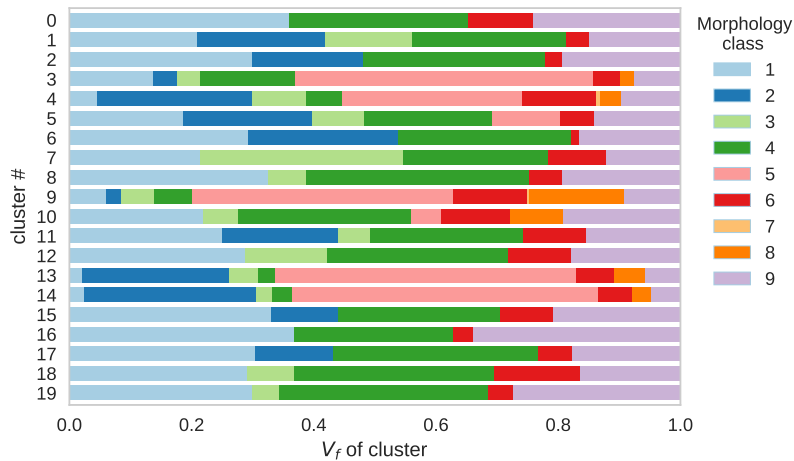


Figure 8: Volume fraction of morphological classes per spatial cluster.

6 REFERENCES

- [1] ASTM. “D2734 - 16: Standard Test Methods for Void Content of Reinforced Plastics”, 2016.
- [2] L. Breiman. “Random forests”. *Machine learning*, vol. 45, no. 1, pp. 5–32, 2001.
- [3] H2O.ai. *Python Interface for H₂O*, 2017.
- [4] T. Kanungo, D. Mount, N. Netanyahu, C. Piatko, R. Silverman et al. “An efficient k-means clustering algorithm: analysis and implementation”. *IEEE Transactions on Pattern Analysis and Machine Intelligence*, vol. 24, no. 7, pp. 881–892, 2002.
- [5] J. B. Kruskal. “Nonmetric multidimensional scaling”. *Psychometrika*, vol. 29, no. 3, pp. 1–27, 1964.
- [6] A. Madra, J. Adrien, E. Maire, P. Breilkopf and F. Trochu. “Quantitative characterization and classification of short fiber geometry in composite reinforcements by X-ray microtomography”. *Composites Part A: Applied Science and Manufacturing*, 2017, In Review.
- [7] A. Madra, N. E. Hajj and M. Benzeggagh. “X-ray microtomography applications for quantitative and qualitative analysis of porosity in woven glass fiber reinforced thermoplastic”. *Composites Science and Technology*, vol. 95, pp. 50–58, 2014.
- [8] A. Madra, F. Trochu and P. Breilkopf. “TUCompframework for modeling and analysis of composite materials based on X-ray microtomography”. In *13ème Colloque National en Calcul des Structures CSMA*, Presqu’île de Giens (Var)2017, pp. 1–8.
- [9] E. Maire and P. J. Withers. “Quantitative X-ray tomography”. *International Materials Reviews*, vol. 59, no. 1, pp. 1–43, 2014.
- [10] F. Pedregosa, G. Varoquaux, A. Gramfort, V. Michel, B. Thirion et al. “Scikit-learn: Machine Learning in Python”. *Journal of Machine Learning Research*, vol. 12, pp. 2825–2830, 2012.
- [11] D. Svozil, V. Kvasnička and J. Pospíchal. “Introduction to multi-layer feed-forward neural networks”. *Chemometrics and Intelligent Laboratory Systems*, vol. 39, no. 1, pp. 43–62, 1997.